Optics Letters

Generation of colorful Airy beams and Airy imaging of letters via two-photon processed cubic phase plates

Ze Cai,[1] Ya Liu,[1] Yanlei Hu,[1,3] Chenchu Zhang,[1] Jiangchuan Xu,[2] Shengyun Ji,[1] Jincheng Ni,[1] Zhaoxin Lao,[1] Jiawen Li,[1] Yang Zhao,[1] Dong Wu,[1,4] and Jiaru Chu[1]

[1]CAS Key Laboratory of Mechanical Behavior and Design of Materials, Department of Precision Machinery and Precision Instrumentation, University of Science and Technology of China, Hefei, Anhui 230027, China
[2]Laboratory of Supervisory Control and Data Acquisition, Department of Precision Machinery and Precision Instrumentation, University of Science and Technology of China, Hefei, Anhui 230027, China
[3]e-mail: huyl@ustc.edu.cn
[4]e-mail: dongwu@ustc.edu.cn

Received 4 January 2018; revised 31 January 2018; accepted 2 February 2018; posted 2 February 2018 (Doc. ID 318963); published 28 February 2018

In this Letter, we demonstrate the observation of colorful Airy beams and Airy imaging of letters, which we called Airy letters here, generated through the continuous cubic phase microplate (CCPP) elaborately fabricated by femtosecond laser two-photon processing. The fabricated CCPP with both micro size (60 μm × 60 μm × 1.1 μm) and continuous variation of phase shows a good agreement with the designed CCPP. Chromatic Airy beams and Airy letters "USTC" are experimentally generated via the CCPP illuminated by white light. In addition, superior properties of Airy letters are explored, demonstrating that the Airy letters inherit the nondiffraction, self-healing, and transverse acceleration characteristics of Airy beams. Our work paves the way toward integrated optics, light separation, optical imaging, and defective information recovery.

OCIS codes: (220.4000) Microstructure fabrication; (100.5090) Phase-only filters; (130.3990) Micro-optical devices; (350.5500) Propagation.

https://doi.org/10.1364/OL.43.001151

Optical light with both gorgeous color and curved shape is a charming phenomenon, and it is common in nature, such as in the rainbow, which is caused by the refraction of the sunlight when it passes through the tiny mist drops in the atmosphere. Recently, a curved beam has been reported, named the Airy beam [1,2], which is a member of nondiffracting waves family [3]. Owing to the intriguing properties of self-bending [4] and self-healing [5], Airy beams have triggered much research in the areas of optical micromanipulation of particles [6,7], generation of curved plasma channels in air [8], surface plasmon control [9,10], laser micromachining of curved structures [11], generation of electron Airy beams [12], and microscopy [13,14]. However, nearly all of these studies rely on monochromatic light, and there is little research on Airy beams in polychromatic light [15,16]; research on Airy beams in different wavelengths in micro size is still a gap to be filled. Furthermore, it has been demonstrated that an image signal can transmit with Airy beams [17], and the signal can be retrieved by performing the Fourier transform. Nevertheless, Airy beams carrying information that can be observed directly (without other transformation) still deserve further study.

From the generation-method point of view, finite Airy beams have been generated experimentally based on cubic phase modulations of Gaussian beams by several techniques using liquid crystal spatial light modulators (SLMs) [1,2], special cylindrical lenses [18,19], and cubic phase masks [8,20]. Nevertheless, phase components in these methods suffer from being macro size, a size not suitable for integrated optics in micro size.

In this Letter, we report the fabrication of continuous cubic phase microplates (CCPPs) by femtosecond laser two-photon processing (TPP), which has proven to be a powerful technique for microfabrication with high efficiency and quality [21–23]. A polychromatic light is separated by the CCPP to generate the colorful Airy beam, and the formation of a colorful Airy beam is thoroughly analyzed. In addition, Airy beams with letter information, so-called Airy letters, are demonstrated, as are their properties.

The envelope of a finite Airy beam [1] is expressed as

$$\phi(\xi, s) = \mathrm{Ai}[s - (\xi/2)^2 + ia\xi] \exp[as - (a\xi^2/2) - i(\xi^3/12) + i(a^2\xi/2) + i(s\xi/2)], \quad (1)$$

where $\mathrm{Ai}[s - (\xi/2)^2 + ia\xi]$ represents the Airy function, a is a positive parameter for ensuring containment of the infinite Airy tail, $a \ll 1$, $s = x/x_0$ represents a dimensionless transverse coordinate, and x_0 is an arbitrary transverse scale. A normalized propagation distance is represented by $= z/kx_0$, and

$k = 2\pi n/\lambda$ is the wavenumber with refractive index of medium n and free-space wavelength λ. For a two-dimensional (2D) case, the Fourier transform of the envelope is proportional to $\exp[i\beta^3(k_x^3 + k_y^3)/3]$, where β is a scale factor and k_x and k_y are Fourier spectrum coordinates. Thus, a plane wave can be converted into an Airy beam by applying a cubic phase modulation followed by a spatial Fourier transformation through focusing with a lens. It is known that the relation between the thickness and accumulated phase is

$$h(x, y) = \frac{\lambda_{in}\varphi(x, y)}{[2\pi(n_m - n_{\text{air}})]}, \tag{2}$$

where λ_{in} is the wavelength of incident light for generating Airy beams and n_m and n_{air} represent the refractive indices of material and air, respectively. Therefore, the cubic phase pattern [Fig. 1(b)], whose size is 600 × 600 pixels, wrapped between 0 and 2π with the phase range varying from -12π to 12π, can be converted into a height profile through Eq. (2). The test lights used in this study are green light (532 nm) and white light (spanning 390–780 nm), thus λ_{in} can be set to 550 nm. The refractive indices of the photoresist (SZ2080) mixed with 1 wt% 4, 4′-Bis(diethylamino)benzophenone (BIS) as photoinitiator and air are ∼1.5 and ∼1, respectively. Therefore, the maximum height is ∼1.1 μm. Figures 1(d) and 1(e) display the scanning electron microscope (SEM) images of the CCPP fabricated by a femtosecond laser TPP (80 MHz repetition rate, 800 nm center wavelength and 75 fs pulse width, and 8 mW exposing power) [Fig. 1(a)], showing a fine fabricating quality

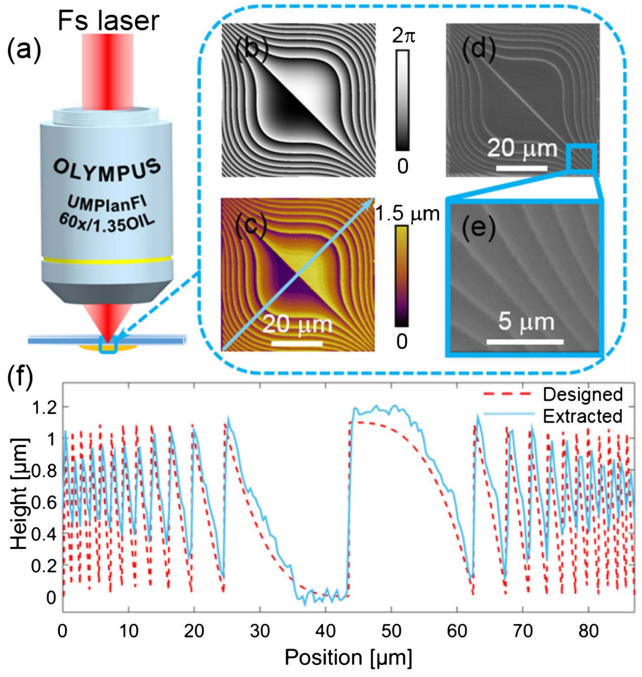

Fig. 1. Fabrication and characterization of CCPPs. (a) Schematic illustration of femtosecond laser TPP CCPPs. (b) Cubic phase pattern wrapped between 0 and 2π. Size, 600 × 600 pixels; phase range, $-12\pi \sim 12\pi$. (c)–(e) AFM, SEM, and locally magnified SEM images of the fabricated CCPP, respectively. (f) Height profile with respect to the substrate (300 nm) along the diagonal line of the CCPP: blue solid line represents the extracted profile marked in (c), and red dashed line represents the designed profile.

[24]. The surface morphology of the CCPP is considered as a significant factor in our fabrication. Hence, the topography of the CCPP was characterized by an atomic force microscope (AFM: MFP3D Origin, Cantilever: Tap300Al-G tapping mode probe). The extracted height profile of the CCPP relative to the substrate (300 nm) along the diagonal marked in Fig. 1(c) is shown in Fig. 1(f), which has a good agreement with the designed height. Some small differences between the designed and the measured height profile may be caused by the fabrication or measurement errors. It is unavoidable in a micrometer/nano scale that some small fluctuations came into being, especially in the center of the CCPP, caused by the distortion of the photoresist during the fabrication and development. It is also necessary to explain that owing to the high aspect ratio of local areas, the AFM probe cannot dip into the bottom, which causes the mismatching between the extracted height and the designed height in the corner of the CCPP.

A continuous-wave laser beam (532 nm, 1 mW), which is truncated through an aperture to ensure the small beam width (∼100 μm) since the length of the CCPP is 60 μm, is transmitted through the fabricated CCPP with a cubic phase modulation. It is then focused by a 40× objective lens (NA = 0.6) with a focal length $f = 180$ μm. The Airy beam is formed at the back focal plane and recorded by a charge-coupled device (CCD) camera after being magnified by a lens group. The intensity pattern of the Airy beam shows the characteristic multilobes [Fig. 2(a)], while the main lobe contains a majority of the total beam energy, which is in good agreement with the simulation [Fig. 2(a) inset: the simulation is operated according to diffraction theory]. When the laser source (monochromatic light) was replaced by a halogen lamp (polychromatic light), a fantastic phenomenon appeared: generation of a colorful Airy beam. Figure 2(b) depicts the colorful Airy beam experimentally observed at the propagation distance of 100 μm after the Fourier plane of the objective lens, which is coincident with the simulated result [Fig. 2(b) inset]. There is also a characteristic intensity pattern of the Airy beam, although the side lobes are blurry.

The formation of Airy beams with multicolor can be explained using the equation of transverse deflection [8]:

$$D(z) = \sqrt{2}\lambda_{in}^2(16\pi^2/x_0^3) \times z^2, \tag{3}$$

where λ_{in} is the wavelength of the incident light to generate Airy beam, x_0 is an arbitrary transverse scale and can be expressed as $x_0 = \beta f\lambda_{in}/(2\pi)$, f is the focal length of the lens for the Fourier transform, z is the propagation distance after the Fourier plane, and the deflection direction is along the 45° axis during the propagation. Therefore, in Eq. (3) the deflection $D(z)$ is proportional to $1/\lambda_{in}$, so the deflection varies when the wavelength of incident light changes at the certain propagation plane. When the CCPP is illuminated by the white light with a broad range of wavelengths, a series of Airy beams with various deflections come into being, and the larger the propagation distance, the stronger the deflection. Figure 2(c) illustrates the transverse acceleration of a colorful Airy beam. Deflections of red, green, and blue elements in a colorful Airy beam were measured at different propagation planes, respectively, and they are in good agreement with the theoretical calculations at the corresponding wavelengths. With the increase of the propagation distance, gaps between different deflections enlarge, so a colorful Airy beam, which is generated

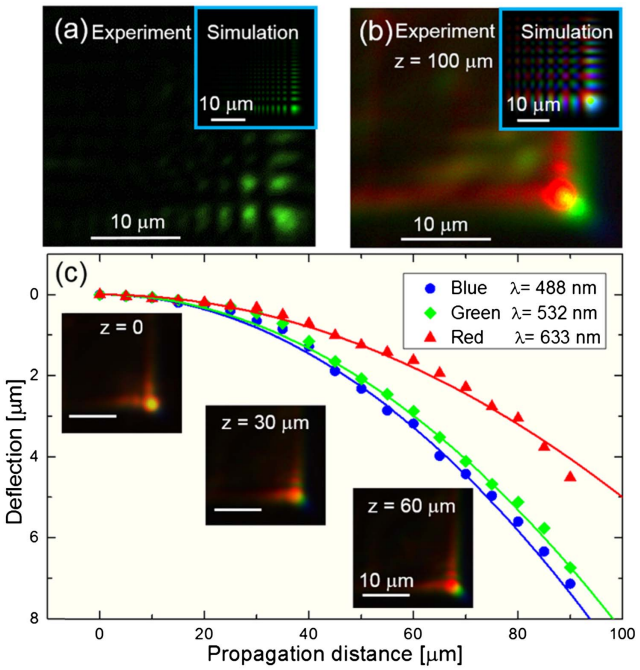

Fig. 2. Observation of colorful Airy beams. (a) A 2D Airy beam generated via the CCPP at the wavelength of 532 nm. Inset: simulation. (b) A colorful Airy beam generated via the CCPP under white light illumination after propagating 100 μm. Inset: a composite image of the simulated results under different wavelengths. (c) Transverse acceleration of the colorful Airy beam generated via the CCPP as a function of beam propagation distance. Red, green, and blue points mark the experimental results separated from the colorful Airy beam, whereas lines in corresponding colors are theoretical calculations. Insets: colorful Airy beams at different propagation distances.

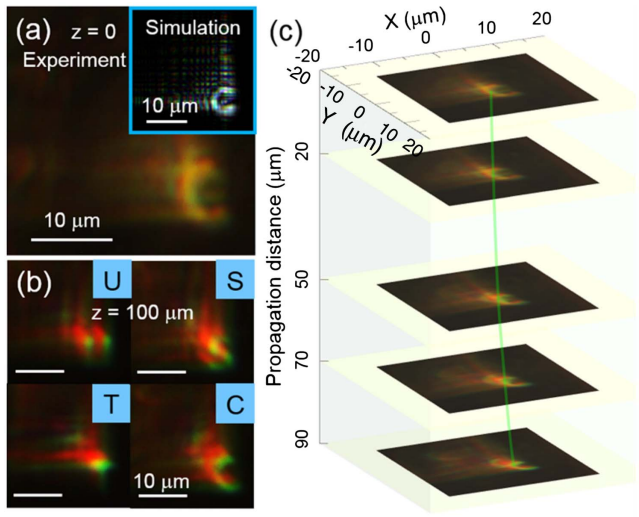

Fig. 3. Observation of Airy letters. (a) An Airy letter "C" generated through the CCPP under white light illumination. Inset: a composite image of the simulated results under different wavelengths. (b) Images of colorful Airy letters "U," "S," "T," "C" after propagating 100 μm. (c) The Airy letter "C" observed at different propagation distances.

from a light but splits during propagation, comes into being [insets in Fig. 2(c)]. However, the photoresist we used shows an absorption band in the spectral range of 450–500 nm [25], so the light loses most of energy in this spectral range after passing through the CCPP. In addition, due to the small gap between the wavelength of green light (532 nm) and blue light (488 nm), their deflection rates differ little. These account for the unobvious blue element in Fig. 2(b). Fortunately, it can be solved by using the same photoresist (SZ2080) without the photoinitiator (BIS) [26]. Therefore, a polychromatic light can be separated to components with different wavelengths through the CCPP. Furthermore, for Airy beams with strong deflection that are micro size [24], they can split quickly in a short distance.

An Airy letter was observed [Fig. 3(a)] when a positive letter mask (the area of letter for transmitting and the other area for blocking) was located after the incident light [Fig. 4(a)]. Other than for reference [17], letter information loaded on the Airy beam can be observed directly without any transformation. As shown in Fig. 4(a), the letter mask "C" (the size of the letter is about 80 μm × 80 μm) is located far from (more than 15 mm) the CCPP. After long-distance diffraction (Fraunhofer diffraction), the letter information (spatial spectrum) is uploaded onto the CCPP on the Fourier plane, which is different from the previous study in which the image signal pattern was uploaded directly onto the cubic phase [17]. The Airy letter is then generated through the Fourier transform of the objective lens. The experimental result [Fig. 3(a)] is consistent with the simulation [Fig. 3(a) inset]. Similar to colorful Airy beams, Airy letters do not present multicolor at or near the Fourier plane of the objective lens, and with the increase of propagation distance, an Airy letter splits into several of the same letters with different colors. After separation, a part of the area of side lobes near the main letter is covered by some Airy letters in long wavelengths (like the Airy letter in red), so the remaining area is blurry and difficult to distinguish. Therefore, unlike the colorful Airy beam [Fig. 2(b)], the colorful Airy letter does not show any clear side lobes, and the whole area of side lobes presents a blur. Figure 3(b) depicts the colorful Airy letters "USTC" at the propagation distance of 100 μm. Under some circumstances, this characteristic of Airy letters can be helpful because there is no need to receive side lobes. Although the multicolors of Airy letters during propagation must be avoided in most imaging applications, it may be useful in multicolor imaging display.

It is evident that colorful Airy beams show the properties of nondiffraction, transverse acceleration, and self-healing. Figure 2(c) illustrates the transverse acceleration property of colorful Airy beams, whereas the insets in Fig. 2(c) account for the nondiffraction character. The spot sizes of colorful Airy beams' main lobes remain almost unchanged at different propagation planes, and the multicolors of Airy beams become obvious gradually during the propagation. Moreover, when the main lobe of a colorful Airy beam is obstructed at the Fourier plane of the objective lens, it is reborn to a great extent after a propagation of 90 μm [inset Fig. 4(a)], revealing its self-healing property.

To explore whether colorful Airy letters possess properties similar to Airy beams, a series of tests has been carried out. Airy letters "U," "S," "T," and "C" were generated and observed at different propagation distances. Figure 3(c) depicts images of the Airy letter "C" at the propagation distances of 0, 20 μm,

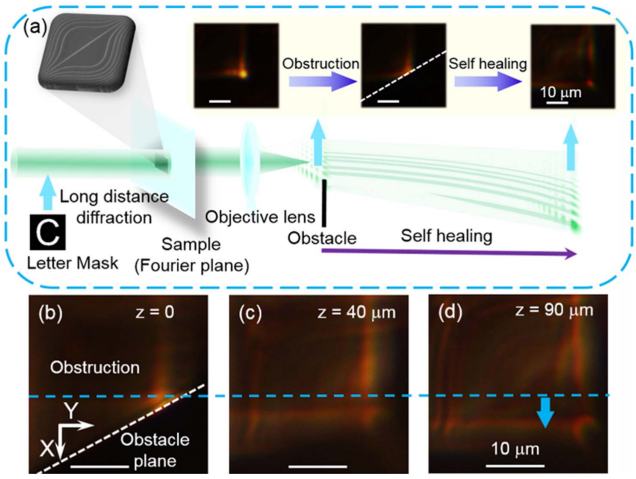

Fig. 4. Self-healing properties of colorful Airy beams and Airy letters. (a) Schematic illustration for investigating the properties of Airy letters. Inset: the reconstruction process of the colorful Airy beam (without the letter mask). (b)–(d) Experimental images of the colorful Airy letter "C" at different propagation planes after it is obstructed.

50 μm, 70 μm, and 90 μm, respectively. The Airy letter keeps its size almost unchanged during a parabolic trajectory with the same deflection in X and Y directions ($x_D = y_D \approx 4$ μm), and the propagation trajectory is marked with the green line. The letter imaging on the main lobe of Airy beam is caused by the combination of the spectrum of letter mask and the cubic phase because the main lobe corresponds to a different part of the spatial spectrum [27], and it accelerates with Airy beam propagating (acceleration of Airy letter). However, when the letter mask (negative mask, the area of letter for blocking and the other area for transmitting) is in the opposite situation, we cannot see the letter image coupled with the Airy beam. Therefore, information imposed on the Airy beam can be observed directly only when the mask is chosen properly. The intensity distribution is related to letter masks and deserves further study. Furthermore, the Airy letter "C" was blocked by a copper wire at the Fourier plane of the objective lens for the verification of the self-healing properties [Fig. 4(b)]. After propagating 40 μm, a fraction of the Airy letter "C" began to repair as shown in Fig. 4(c). Further propagation made the Airy letter fully recover its original shape [Fig. 4(d)]. As a consequence, Airy letters are revealed to inherit the nondiffraction, transverse acceleration, and self-healing properties of Airy beams.

In conclusion, we have presented a cubic phase component CCPP with both micro size and continuous variation of phase that can be valuable in integrated micro-optics. Colorful Airy beams and Airy letters have been generated experimentally through the fabricated CCPP. The formation of Airy beams with multicolor has been analyzed systematically, and the properties of colorful Airy beams and Airy letters have been explored as well. As demonstrated in our experiments, colorful Airy beams and Airy letters are similar to monochromatic Airy beams, possessing the properties of nondiffraction, transverse acceleration, and self-healing. The research on colorful Airy beams may provide a new way for light separation through the generation of accelerating beams, and the study of Airy letters may create a new platform for research in imaging science, defective information recovery, and even other, undiscovered territories.

Funding. National Natural Science Foundation of China (NSFC) (51405464, 51605463, 51675503, 61475149, 61675190); Fundamental Research Funds for the Central Universities (WK2090000011, WK2480000002); Youth Innovation Promotion Association of the Chinese Academy of Sciences (2017495).

REFERENCES

1. G. A. Siviloglou, J. Broky, A. Dogariu, and D. N. Christodoulides, Phys. Rev. Lett. **99**, 213901 (2007).
2. G. A. Siviloglou and D. N. Christodoulides, Opt. Lett. **32**, 979 (2007).
3. M. V. Berry and N. L. Balazs, Am. J. Phys. **47**, 264 (1979).
4. G. A. Siviloglou, J. Broky, A. Dogariu, and D. N. Christodoulides, Opt. Lett. **33**, 207 (2008).
5. J. Broky, G. A. Siviloglou, A. Dogariu, and D. N. Christodoulides, Opt. Express **16**, 12880 (2008).
6. J. Baumgartl, M. Mazilu, and K. Dholakia, Nat. Photonics **2**, 675 (2008).
7. P. Zhang, J. Prakash, Z. Zhang, M. S. Mills, N. K. Efremidis, D. N. Christodoulides, and Z. Chen, Opt. Lett. **36**, 2883 (2011).
8. P. Polynkin, M. Kolesik, J. V. Moloney, G. A. Siviloglou, and D. N. Christodoulides, Science **324**, 229 (2009).
9. A. Minovich, A. E. Klein, N. Janunts, T. Pertsch, D. N. Neshev, and Y. S. Kivshar, Phys. Rev. Lett. **107**, 116802 (2011).
10. A. Salandrino and D. N. Christodoulides, Opt. Lett. **35**, 2082 (2010).
11. A. Mathis, F. Courvoisier, L. Froehly, L. Furfaro, M. Jacquot, P. A. Lacourt, and J. M. Dudley, Appl. Phys. Lett. **101**, 071110 (2012).
12. N. Voloch-Bloch, Y. Lereah, Y. Lilach, A. Gover, and A. Arie, Nature **494**, 331 (2013).
13. S. Jia, J. C. Vaughan, and X. Zhuang, Nat. Photonics **8**, 302 (2014).
14. T. Vettenburg, H. I. C. Dalgarno, J. Nylk, C. Coll-Llado, D. E. K. Ferrier, T. Cizmar, F. J. Gunn-Moore, and K. Dholakia, Nat. Methods **11**, 541 (2014).
15. J. E. Morris, M. Mazilu, J. Baumgartl, T. Cizmar, and K. Dholakia, Proc. SPIE **7430**, 74300W (2009).
16. J. E. Morris, M. Mazilu, J. Baumgartl, T. Čižmár, and K. Dholakia, Opt. Express **17**, 13236 (2009).
17. Y. Liang, Y. Hu, D. Song, C. Lou, X. Zhang, Z. Chen, and J. Xu, Opt. Lett. **40**, 5686 (2015).
18. D. G. Papazoglou, S. Suntsov, D. Abdollahpour, and S. Tzortzakis, Phys. Rev. A **81**, 061807 (2010).
19. A. Valdmann, P. Piksarv, H. Valtna-Lukner, and P. Saari, Opt. Lett. **39**, 1877 (2014).
20. R. Cao, Y. Yang, J. Wang, J. Bu, M. Wang, and X. Yuan, Appl. Phys. Lett. **99**, 261106 (2011).
21. M. Malinauskas, A. Žukauskas, S. Hasegawa, Y. Hayasaki, V. Mizeikis, R. Buividas, and S. Juodkazis, Light: Sci. Appl. **5**, e16133 (2016).
22. T. Gissibl, S. Thiele, A. Herkommer, and H. Giessen, Nat. Photonics **10**, 554 (2016).
23. X. Wang, A. A. Kuchmizhak, E. Brasselet, and S. Juodkazis, Appl. Phys. Lett. **110**, 181101 (2017).
24. Z. Cai, Y. Liu, C. Zhang, J. Xu, S. Ji, J. Ni, J. Li, Y. Hu, D. Wu, and J. Chu, Opt. Lett. **42**, 2483 (2017).
25. A. Ovsianikov, J. Viertl, B. Chichkov, M. Oubaha, B. MacCraith, I. Sakellari, A. Giakoumaki, D. Gray, M. Vamvakaki, M. Farsari, and C. Fotakis, ACS Nano **2**, 2257 (2008).
26. L. Jonušauskas, D. Gailevičius, L. Mikoliūnaitė, D. Sakalauskas, S. Šakirzanovas, S. Juodkazis, and M. Malinauskas, Materials **10**, 12 (2017).
27. Y. Hu, D. Bongiovanni, Z. Chen, and R. Morandotti, Phys. Rev. A **88**, 043809 (2013).